Revised paper submitted to the International Journal of Fracture, February 2001.

Three-Dimensional Mixed Mode Analysis of A Cracked Body by Fractal Finite Element Method

R. K. L. Su[a,1]
Ph.D. Assistant Professor

A. Y. T. Leung[b]
D.Sc., Ph.D. Professor, Head of Department

[a] Department of Civil Engineering, University of Hong Kong, Pokfulam Road, Hong Kong

[b] Department of Building and Construction Engineering, City University of Hong Kong, Tat Chee Avenue, Hong Kong

[1] Corresponding Author: Fax (852) 2559 5337

Total Number of Pages: 31

Number of Tables: 2

Number of Figures: 7

Abstract-A semi-analytical method namely fractal finite element method is presented for the determination of stress intensity factor for the straight three-dimenisonal plane crack. Using the concept of fractal geometry, infinite many of finite elements are generated virtually around the crack border. Based on the analytical global displacement function, numerous DOFs are transformed to a small set of generalised coordinates in an expeditious way. No post-processing and special finite elements are required to develop for extracting the stress intensity factors. Examples are given to illustrate the accuracy and efficiency of the present method. Very good accuracy (with less than 3% errors) is obtained for the maximum value of SIFs for different modes.

1. INTRODUCTION

The stress intensity factor (SIF) is an important parameter in fracture mechanics. It has been widely applied on design of pressure vessels, power generation equipment, structures, aircraft and bio-medical devices[1]. The numerical methods of determining SIFs of three-dimensional crack geometry has been receiving more attention because most cracks are three-dimensional in nature and the computer advancements enable the researchers and engineers to evaluate the complexity nature of those cracks. Practicing engineers usually prefer those user-friendly numerical methods with the least computational memory and execution time. The accuracy of about 5% is usually acceptable for most of the engineering analysis.

The comprehensive reviews about the computational method to obtain SIFs are given in [2-4]. Several approaches have been used to determine the SIFs in solids and plates including those requiring the post-processing techniques such as the invariant integrals techniques [5-7], the rate of energy releasing methods [8-10], the weight function methods[11 and 12], the alternating method[13]. However, some methods have been suggested that do not require post-processing thus more attractive. Such examples include the singular stress element[14] for finite element and the special crack tip element[15] for boundary element method.

In this paper, a computational procedure to determine the SIFs of straight crack namely fractal finite element method(FFEM) is presented. The FFEM had been developed recently [16,17] for solving two-dimensional cracks. The advantages of the proposed method are:

i) Using the concept of fractal geometry, infinite finite elements are generated virtually around the crack border. Hence the effort for data preparation can be minimised.

ii) Based on the eigenfunction expansion of the displacement fields along the semi-infinite straight edge crack [18], the infinite many finite elements that generate virtually by fractal geometry around the crack border are transformed by the expeditious manner. Small computational time and tiny memory requirement can be achieved

iii) No special finite elements and post-processing are needed to determine the SIF.

iv) As the analytical solution is embodied in the transformation, the accuracy of SIF is high.

2. GLOBAL DISPLACEMENT INTERPOLATION FUNCTIONS

2.1. Eigenfunction expansions for three-dimensional crack

It was Hartranft *et al* [18] who first conceived the idea of eigenfunction expansion and employed it to analyse the three-dimensional infinite crack problem. The resulting eigenfuntion series expansion is a very precise global interpolation function for displacements near the crack front. In this section, the method of eigenfunction expansion to analyse the elastic three-dimensional crack will be discussed. At the end of this section the complete form of the displacement series will be derived and presented. Since the primary interest in the solution to the crack problem is centred on the disturbances local to the leading edge of the crack, cylindrical coordinate system (r, θ, z) is selected to exhibit the singular character of the stresses in a natural manner.

Consider an infinitely extended elastic solid that contains a crack as a half-plane with the z-axis along the crack edge. The sides of the crack coincide with the surfaces $\theta=\pm\pi$, where

$$0 \le r < \infty, \quad -\pi \le \theta \le \pi, \quad -\infty < z < \infty.$$

By using the linear theory of elasticity, the equations of equilibrium in cylindrical coordinates must be solved for the displacement components (u_r, v_θ, w_z):

$$\begin{aligned}
&\frac{\partial \vartheta}{\partial r} + (1-2\nu)\left[\left(\nabla^2 - \frac{1}{r^2}\right)u_r - \frac{2}{r^2}\frac{\partial v_\theta}{\partial \theta}\right] = 0,\\
&\frac{1}{r}\frac{\partial \vartheta}{\partial \theta} + (1-2\nu)\left[\left(\nabla^2 - \frac{1}{r^2}\right)v_\theta + \frac{2}{r^2}\frac{\partial u_r}{\partial \theta}\right] = 0,\\
&\frac{\partial \vartheta}{\partial z} + (1-2\nu)\nabla^2 w_z = 0.
\end{aligned} \tag{1}$$

In equations (1), ν is Poisson's ratio, ϑ is the dilatation given by

$$\vartheta = \frac{\partial u_r}{\partial r} + \frac{1}{r}\frac{\partial v_\theta}{\partial \theta} + \frac{u_r}{r} + \frac{\partial w_z}{\partial z},$$

and the Laplace operator is defined as

$$\nabla^2 = \frac{\partial^2}{\partial r^2} + \frac{1}{r}\frac{\partial}{\partial r} + \frac{1}{r^2}\frac{\partial^2}{\partial \theta^2} + \frac{\partial^2}{\partial z^2}.$$

The boundary conditions are written in terms of the stresses, which are related to the displacements through the Hooke's law for an isotropic body:

$$\sigma_r = \lambda\vartheta + 2\mu\frac{\partial u_r}{\partial r},$$

$$\sigma_\theta = \lambda\vartheta + 2\mu\left(\frac{1}{r}\frac{\partial v_\theta}{\partial\theta} + \frac{u_r}{r}\right),$$

$$\sigma_z = \lambda\vartheta + 2\mu\frac{\partial w_z}{\partial z}, \tag{2}$$

$$\tau_{r\theta} = \mu\left(\frac{1}{r}\frac{\partial u_r}{\partial\theta} - \frac{v_\theta}{r} + \frac{\partial v_\theta}{\partial r}\right),$$

$$\tau_{\theta z} = \mu\left(\frac{\partial v_\theta}{\partial z} + \frac{1}{r}\frac{\partial w_z}{\partial\theta}\right),$$

$$\tau_{zr} = \mu\left(\frac{\partial w_z}{\partial r} + \frac{\partial u_r}{\partial z}\right),$$

The Lame's coefficients are denoted by λ and μ.

To solve equation (1) under the present boundary conditions

$$\sigma_\theta = \tau_{\theta r} = \tau_{\theta z} = 0 \quad \text{for } \theta = \pm\pi \tag{3}$$

we follow Hartranft[18] and assume the displacement vector in the product form

$$2\mu\mathbf{u} = r^{\beta+n}\mathbf{U}_n(\theta, z; \beta) \quad , \tag{4}$$

where β is the eigenvalues as powers of r and $\mathbf{U}_n$ (U_n, V_n, W_n) are functions of θ and z only.

By inserting the displacement equation (4) into the set of equilibrium equations (1), three simultaneous partial differential equations in three unknown functions $\mathbf{U}_n$ can be sought.

$$\begin{aligned}
&(1-2\nu)\frac{\partial^2 U_n}{\partial\theta^2} + 2(1-\nu)[(\beta+n)^2 - 1]U_n + (\beta+n-3+4\nu)\frac{\partial V_n}{\partial\theta} = \\
&-(\beta+n-1)\frac{\partial W_{n-1}}{\partial z} - (1-2\nu)\frac{\partial^2 U_{n-2}}{\partial z^2} \\
&(\beta+n+3-4\nu)\frac{\partial U_n}{\partial\theta} + 2(1-\nu)\frac{\partial^2 V_n}{\partial\theta^2} + (1-2\nu)[(\beta+n)^2 - 1]V_n = \\
&(2\nu-1)\frac{\partial^2 V_{n-2}}{\partial^2 z} - \frac{\partial^2 W_{n-1}}{\partial\theta\partial z} \\
&(1-2\nu)[(\beta+n)^2 W_n + \frac{\partial^2 W_n}{\partial\theta^2}] = -(1+\beta+n)\frac{\partial U_{n-1}}{\partial z} - \frac{\partial^2 V_{n-1}}{\partial\theta\partial z} - 2(1-\nu)\frac{\partial^2 W_{n-2}}{\partial z^2}
\end{aligned} \tag{5}$$

Equations(5) may yield a recurrence relation expressing $\mathbf{U}_n$ in terms of their previous values.

To solve equations(5), let us consider the first term n=0, the solution takes the form

$$
\begin{aligned}
U_0 &= b_{01}(z)\cos(\beta+1)\theta + b_{02}(z)\sin(\beta+1)\theta \\
&\quad + c_{01}(z)\cos(\beta-1)\theta + c_{02}(z)\sin(\beta-1)\theta, \\
V_0 &= -b_{01}(z)\sin(\beta+1)\theta + b_{02}(z)\cos(\beta+1)\theta \\
&\quad + \frac{\beta+3-4\nu}{\beta-3+4\nu}[-c_{01}(z)\sin(\beta-1)\theta + c_{02}(z)\cos(\beta-1)\theta \\
W_0 &= a_{01}(z)\cos(\beta\theta) + a_{02}(z)\sin(\beta\theta)
\end{aligned} \tag{6}
$$

where a_{0i}, b_{0i} and c_{0i} (i=1,2) are arbitrary functions of z. Without loss in generality, β can be determined by applying the boundary conditions (3) and stresses equation (2). One can have six conditions to solve for the six unknown functions a_{0i}, b_{0i} and c_{0i} (i=1,2), for a non-trivial solution, the determinant of the coefficients of these functions must vanish, and hence β are found to be the roots of the characteristic-value equation

$$\sin(2\pi\beta) = 0$$

which has only real roots

$$\beta = \frac{n}{2} \qquad n=0,1,2,... \tag{7}$$

The negative values of n have been excluded in equation (7) as negative β will result in the unacceptable singularities. Hence by adding up the n displacements vector equation (4) the complete displacement vector become

$$2\mu\mathbf{u} = \sum_{n=0}^{\infty} r^{n/2}\mathbf{F}_n(\theta, z). \tag{8}$$

where $\mathbf{F}_n$ (f_n, g_n, h_n) are functions of θ and z only. For the same incentive, the expressions for the stresses in equations (2) may be simplified and they become

$$
\begin{aligned}
(1-2\nu)\sigma_r &= \sum_{n=0}^{\infty} r^{n/2-1}\left\{\left[\frac{n}{2}-\left(\frac{n}{2}-1\right)\nu\right]f_n + \nu\left[\frac{\partial g_n}{\partial\theta} + \frac{\partial h_{n-2}}{\partial z}\right]\right\}, \\
(1-2\nu)\sigma_\theta &= \sum_{n=0}^{\infty} r^{n/2-1}\left\{\left[1-\left(\frac{n}{2}-1\right)\nu\right]f_n + (1-\nu)\frac{\partial g_n}{\partial\theta} + \nu\frac{\partial h_{n-2}}{\partial z}\right\}, \\
(1-2\nu)\sigma_z &= \sum_{n=0}^{\infty} r^{n/2-1}\left\{\nu\left[\left(\frac{n}{2}+1\right)f_n + \frac{\partial g_n}{\partial\theta}\right] + (1-\nu)\frac{\partial h_{n-2}}{\partial z}\right\}, \\
2\tau_{r\theta} &= \sum_{n=0}^{\infty} r^{n/2-1}\left[\frac{\partial f_n}{\partial\theta} + \left(\frac{n}{2}-1\right)g_n\right],
\end{aligned} \tag{9}
$$

$$2\tau_{\theta z} = \sum_{n=0}^{\infty} r^{n/2-1}\left(\frac{\partial h_n}{\partial \theta} + \frac{\partial g_{n-2}}{\partial z}\right),$$

$$2\tau_{zr} = \sum_{n=0}^{\infty} r^{n/2-1}\left(\frac{n}{2}h_n + \frac{\partial f_{n-2}}{\partial z}\right),$$

Similarly the set of simultaneous partial differential equations (5) are simplified to the form of

$$\begin{aligned}
&(1-2\nu)\frac{\partial^2 f_n}{\partial \theta^2} + 2(1-\nu)\left(\frac{n^2}{4}-1\right)f_n + \left(\frac{n}{2}-3+4\nu\right)\frac{\partial g_n}{\partial \theta} = \\
&-\left(\frac{n}{2}-1\right)\frac{\partial h_{n-2}}{\partial z} - (1-2\nu)\frac{\partial^2 f_{n-4}}{\partial z^2} \\
&2(1-\nu)\frac{\partial^2 g_n}{\partial \theta^2} + (1-2\nu)\left(\frac{n^2}{4}-1\right)g_n + \left(\frac{n}{2}+3-4\nu\right)\frac{\partial f_n}{\partial \theta} = \\
&-\frac{\partial^2 h_{n-2}}{\partial \theta \partial z} - (1-2\nu)\frac{\partial^2 g_{n-4}}{\partial z^2} \\
&(1-2\nu)\left(\frac{\partial^2 h_n}{\partial \theta^2} + \frac{n^2}{4}h_n\right) = -\frac{n}{2}\frac{\partial f_{n-2}}{\partial z} - \frac{\partial^2 g_{n-2}}{\partial \theta \partial z} - 2(1-\nu)\frac{\partial^2 h_{n-4}}{\partial z^2}.
\end{aligned} \qquad (10)$$

After solving equation (10) a general set of displacement solutions can be obtained. By applying the boundary conditions (3), one can get the relationship between a_{n1} *and* a_{n2} or b_{n1} *and* b_{n2} or c_{n1} *and* c_{n2} in equation(8). Without go into details, the complete global transformation function $\mathbf{F}_n$ are evaluated up to the eighth term as it had shown to be converged[20]. The results are listed out as the following,

For n=0, (the arbitrary function is changed from $4(1\text{-}\nu)a_0^{(i)}$ to $a_0^{(i)}$, i=1,2)

$$f_0 = a_0^{(1)}\cos\theta + a_0^{(2)}\sin\theta$$

$$g_0 = -a_0^{(1)}\sin\theta + a_0^{(2)}\cos\theta$$

$$h_0 = a_0^{(3)}$$

For n=1

$$\begin{aligned}
f_1 &= a_1^{(1)}\left[\cos\frac{3\theta}{2} - (5-8\nu)\cos\frac{\theta}{2}\right] \\
&\quad + a_1^{(2)}\left[\sin\frac{3\theta}{2} - \frac{(5-8\nu)}{3}\sin\frac{\theta}{2}\right]
\end{aligned}$$

$$g_1 = -a_1^{(1)}\left[\sin\frac{3\theta}{2} - (7-8\nu)\sin\frac{\theta}{2}\right] + a_1^{(2)}\left[\cos\frac{3\theta}{2} - \frac{(7-8\nu)}{3}\cos\frac{\theta}{2}\right]$$

$$h_1 = a_1^{(3)}\sin\frac{\theta}{2}$$

For n=2

$$f_2 = a_2^{(1)}[\cos 2\theta + 1 - 2\nu] - a_0^{(3)'}\nu$$

$$g_2 = -a_2^{(1)}\sin 2\theta + a_2^{(2)}$$

$$h_2 = a_2^{(3)}\cos\theta - a_0^{(2)'}\sin\theta$$

For n=3

$$f_3 = a_3^{(1)}\left[\cos\frac{5\theta}{2} + (3-8\nu)\cos\frac{\theta}{2}\right] + a_3^{(2)}\left[\sin\frac{5\theta}{2} + \frac{(3-8\nu)}{5}\sin\frac{\theta}{2}\right] - a_1^{(3)'}\frac{2}{15}(1+4\nu)\sin\frac{\theta}{2}$$

$$g_3 = -a_3^{(1)}\left[\sin\frac{5\theta}{2} - (9-8\nu)\sin\frac{\theta}{2}\right] + a_3^{(2)}\left[\cos\frac{5\theta}{2} - \frac{(9-8\nu)}{5}\cos\frac{\theta}{2}\right] - a_1^{(3)'}\frac{4}{15}(1-2\nu)\cos\frac{\theta}{2}$$

$$h_3 = a_3^{(3)}\sin\frac{3\theta}{2} - 2a_1^{(1)'}\left[\frac{(7-8\nu)}{3}\cos\frac{3\theta}{2} - \cos\frac{\theta}{2}\right] + \frac{2}{3}a_1^{(2)'}\sin\frac{\theta}{2}$$

For n=4

$$f_4 = a_4^{(1)}\left[\cos 3\theta + \frac{(1-4\nu)}{3}\cos\theta\right] + a_4^{(2)}\left[\sin 3\theta + (1-4\nu)\sin\theta\right] - a_2^{(3)'}\frac{(1+2\nu)}{6}\cos\theta - a_0^{(1)''}\frac{(1-\nu)}{6}\cos\theta + a_0^{(2)''}\frac{\nu}{2}\sin\theta$$

$$g_4 = -a_4^{(1)}\left[\sin 3\theta - \frac{(5-4\nu)}{3}\sin\theta\right] + a_4^{(2)}\left[\cos 3\theta - (5-4\nu)\cos\theta\right] + a_2^{(3)'}\frac{(1-2\nu)}{6}\sin\theta + a_0^{(1)''}\frac{(1+\nu)}{6}\sin\theta - a_0^{(2)''}\frac{\nu}{2}\cos\theta$$

$$h_4 = a_4^{(3)}\cos 2\theta - a_2^{(2)'}\frac{1}{2}\sin 2\theta - a_2^{(1)'}\frac{1}{2} - a_0^{(1)''}\frac{1}{2}$$

For n=5

$$f_5 = a_5^{(1)}\left[\cos\frac{7\theta}{2} + \frac{(1-8\nu)}{3}\cos\frac{3\theta}{2}\right] + a_5^{(2)}\left[\sin\frac{7\theta}{2} + \frac{(1-8\nu)}{7}\sin\frac{3\theta}{2}\right]$$
$$- a_3^{(3)\prime}\frac{(6+8\nu)}{35}\sin\frac{3\theta}{2}$$
$$+ a_1^{(1)\prime\prime}\left[\frac{(61+32\nu-128\nu^2)}{90}\cos\frac{3\theta}{2} + \frac{(1-8\nu)}{6}\cos\frac{\theta}{2}\right]$$
$$- a_1^{(2)\prime\prime}\left[\frac{(77-128\nu+128\nu^2)}{630}\sin\frac{3\theta}{2} - \frac{(1-8\nu)}{9}\sin\frac{\theta}{2}\right]$$

$$g_5 = -a_5^{(1)}\left[\sin\frac{7\theta}{2} - \frac{(11-8\nu)}{3}\sin\frac{3\theta}{2}\right] + a_5^{(2)}\left[\cos\frac{7\theta}{2} - \frac{(11-8\nu)}{7}\cos\frac{3\theta}{2}\right]$$
$$- a_3^{(3)\prime}\frac{(4-8\nu)}{35}\cos\frac{3\theta}{2}$$
$$- a_1^{(1)\prime\prime}\left[\frac{(49-192\nu+128\nu^2)}{90}\sin\frac{3\theta}{2} + \frac{(7-8\nu)}{6}\sin\frac{\theta}{2}\right]$$
$$+ a_1^{(2)\prime\prime}\left[\frac{(7-228\nu+128\nu^2)}{630}\cos\frac{3\theta}{2} + \frac{(7-8\nu)}{9}\cos\frac{\theta}{2}\right]$$

$$h_5 = a_5^{(3)}\sin\frac{5\theta}{2} - a_3^{(1)\prime}\left[2\cos\frac{\theta}{2} - \frac{(18-16\nu)}{5}\cos\frac{5\theta}{2}\right]$$
$$- b_3^{(2)\prime}\frac{2}{5}\sin\frac{\theta}{2} - a_1^{(3)\prime\prime}\frac{3}{10}\sin\frac{\theta}{2}$$

For n=6

$$f_6 = a_6^{(1)}[\cos 4\theta - \nu\cos 2\theta] + a_6^{(2)}[\sin 4\theta - 2\nu\sin 2\theta]$$
$$- a_4^{(3)\prime}\frac{(1+\nu)}{6}\cos 2\theta + a_2^{(1)\prime\prime}\left[\frac{\nu}{4} - \frac{(1-\nu+\nu^2)}{12}\cos 2\theta\right]$$
$$+ a_2^{(2)\prime\prime}\frac{(1+\nu)}{12}\sin 2\theta + a_0^{(3)\prime\prime\prime}\frac{1}{48}[3+6\nu+\nu(1-2\nu)\cos 2\theta]$$

$$g_6 = -a_6^{(1)}\left[\sin 4\theta - \frac{(3-2\nu)}{2}\sin 2\theta\right] + a_6^{(2)}\left[\cos 4\theta - (3-2\nu)\cos 2\theta\right]$$
$$- a_4^{(3)\prime}\frac{(1-2\nu)}{12}\sin 2\theta + a_2^{(1)\prime\prime}\left[\frac{(1+5\nu-2\nu^2)}{24}\sin 2\theta\right]$$
$$- a_2^{(2)\prime\prime}\frac{1}{24}\left[3-(1-2\nu)\cos 2\theta\right] - a_0^{(3)\prime\prime\prime}\frac{1}{96}(3-8\nu+4\nu^2)\sin 2\theta$$

$$h_6 = a_6^{(1)}\cos 3\theta - a_4^{(1)\prime}\frac{1}{3}\cos\theta - a_4^{(2)\prime}\left[\sin\theta - \frac{(5-4\nu)}{3}\sin 3\theta\right]$$
$$- a_2^{(3)\prime\prime}\frac{5}{24}\cos\theta + a_0^{(1)\prime\prime\prime}\frac{1}{24}\cos\theta + a_0^{(2)\prime\prime\prime}\left[\frac{1}{4}\sin\theta - \frac{(1-2\nu)}{12}\sin 3\theta\right]$$

For n=7

$$f_7 = a_7^{(1)}\left[\cos\frac{9\theta}{2} - \frac{(1+8\nu)}{5}\cos\frac{5\theta}{2}\right] + a_7^{(2)}\left[\sin\frac{9\theta}{2} - \frac{(1+8\nu)}{9}\sin\frac{5\theta}{2}\right]$$
$$- a_5^{(3)\prime}\frac{(10+8\nu)}{63}\sin\frac{5\theta}{2}$$
$$+ a_3^{(1)\prime\prime}\left[\frac{(1+8\nu)}{10}\cos\frac{\theta}{2} - \frac{(223-32\nu-128\nu^2)}{350}\cos\frac{5\theta}{2}\right]$$
$$+ a_3^{(2)\prime\prime}\left[\frac{(3+24\nu)}{150}\sin\frac{\theta}{2} - \frac{(207-128\nu+128\nu^2)}{3150}\sin\frac{5\theta}{2}\right]$$
$$+ a_1^{(3)\prime\prime\prime}\left[\frac{(3+4\nu)}{75}\sin\frac{\theta}{2} + \frac{(4+24\nu-64\nu^2)}{4725}\sin\frac{5\theta}{2}\right]$$

$$g_7 = -a_7^{(1)}\left[\sin\frac{9\theta}{2} - \frac{(13-8\nu)}{5}\sin\frac{5\theta}{2}\right] + a_7^{(2)}\left[\cos\frac{9\theta}{2} - \frac{(13-8\nu)}{9}\cos\frac{5\theta}{2}\right]$$
$$- a_5^{(3)\prime}\frac{(4-8\nu)}{63}\cos\frac{5\theta}{2}$$
$$+ a_3^{(1)\prime\prime}\left[\frac{(-9+8\nu)}{10}\sin\frac{\theta}{2} + \frac{(99-192\nu+128\nu^2)}{350}\sin\frac{5\theta}{2}\right]$$
$$+ a_3^{(2)\prime\prime}\left[\frac{(27-24\nu)}{150}\cos\frac{\theta}{2} - \frac{(171+352\nu-128\nu^2)}{3150}\cos\frac{5\theta}{2}\right]$$
$$+ a_1^{(3)\prime\prime\prime}\left[\frac{(2-4\nu)}{75}\cos\frac{\theta}{2} + \frac{(52-136\nu+64\nu^2)}{4725}\cos\frac{5\theta}{2}\right]$$

$$h_7 = a_7^{(3)}\sin\frac{7\theta}{2} + a_5^{(1)\prime}\left[-\frac{2}{3}\cos\frac{3\theta}{2} + \frac{(22-16\nu)}{21}\cos\frac{7\theta}{2}\right]$$
$$- a_5^{(2)\prime}\frac{2}{7}\sin\frac{3\theta}{2} - a_3^{(3)\prime\prime}\frac{11}{70}\sin\frac{3\theta}{2}$$
$$- a_1^{(1)\prime\prime\prime}\left[\frac{1}{3}\cos\frac{\theta}{2} - \frac{(7-8\nu)}{9}\cos\frac{3\theta}{2} + \frac{(64-192\nu+128\nu^2)}{315}\cos\frac{7\theta}{2}\right]$$
$$- a_1^{(2)\prime\prime\prime}\left[\frac{1}{9}\sin\frac{\theta}{2} - \frac{(14-16\nu)}{315}\sin\frac{3\theta}{2}\right]$$

For n=8

$$
\begin{aligned}
f_8 &= a_8^{(1)}\left[\cos 5\theta - \frac{(1+4\nu)}{5}\cos 3\theta\right] + a_8^{(2)}\left[\sin 5\theta - \frac{(1+4\nu)}{3}\sin 3\theta\right] \\
&\quad - a_6^{(3)\prime}\,\frac{(3+2\nu)}{20}\cos 3\theta \\
&\quad + a_4^{(1)\prime\prime}\left[\frac{(-5+2\nu-2\nu^2)}{90}\cos 3\theta + \frac{(1+4\nu)}{36}\cos\theta\right] \\
&\quad + a_4^{(2)\prime\prime}\left[\frac{(-11+2\nu+4\nu^2)}{36}\sin 3\theta + \frac{(1+4\nu)}{12}\sin\theta\right] \\
&\quad + a_2^{(3)\prime\prime\prime}\left[\frac{(1+2\nu-8\nu^2)}{1440}\cos 3\theta + \frac{(1+\nu)}{36}\cos\theta\right] \\
&\quad + a_0^{(1)\prime\prime\prime\prime}\left[\frac{(-1-2\nu+8\nu^2)}{2880}\cos(3\theta) + \frac{(1-8\nu)}{576}\cos\theta\right] \\
&\quad + a_0^{(1)\prime\prime\prime\prime}\left[\frac{(7-10\nu-8\nu^2)}{576}\sin(3\theta) - \frac{(5+8\nu)}{192}\sin\theta\right]
\end{aligned}
$$

$$
\begin{aligned}
g_8 &= -a_8^{(1)}\left[\sin 5\theta - \frac{(7-4\nu)}{5}\sin 3\theta\right] + a_8^{(2)}\left[\cos 5\theta - \frac{(7-4\nu)}{3}\cos 3\theta\right] \\
&\quad - a_6^{(3)\prime}\,\frac{(1-2\nu)}{20}\sin 3\theta \\
&\quad + a_4^{(1)\prime\prime}\left[\frac{(5+6\nu-2\nu^2)}{90}\sin 3\theta + \frac{(-5+4\nu)}{36}\sin\theta\right] \\
&\quad + a_4^{(2)\prime\prime}\left[\frac{(-5+6\nu-4\nu^2)}{36}\cos 3\theta + \frac{(5-4\nu)}{12}\cos\theta\right] \\
&\quad + a_2^{(3)\prime\prime\prime}\left[\frac{(-7+18\nu-8\nu^2)}{1440}\sin 3\theta + \frac{(-1+2\nu)}{72}\sin\theta\right] \\
&\quad + a_0^{(1)\prime\prime\prime\prime}\left[\frac{(7-18\nu+8\nu^2)}{2880}\sin(3\theta) - \frac{(5+8\nu)}{576}\sin\theta\right] \\
&\quad + a_0^{(1)\prime\prime\prime\prime}\left[\frac{(1-6\nu+8\nu^2)}{576}\cos(3\theta) + \frac{(-1+8\nu)}{192}\cos\theta\right]
\end{aligned}
$$

$$
\begin{aligned}
h_8 &= a_8^{(1)}\cos 4\theta - a_6^{(1)\prime}\,\frac{1}{4}\cos 2\theta + a_6^{(2)\prime}\left[\frac{(3-2\nu)}{4}\sin 4\theta - \frac{1}{2}\sin 2\theta\right] \\
&\quad - a_4^{(3)\prime\prime}\,\frac{1}{8}\cos 2\theta + a_2^{(1)\prime\prime\prime}\left[\frac{1}{16} + \frac{(1-\nu)}{48}\cos 2\theta\right] \\
&\quad + a_2^{(2)\prime\prime\prime}\left[\frac{1}{16}\sin 2\theta + \frac{(-1+2\nu)}{96}\sin 4\theta\right] + a_0^{(3)\prime\prime\prime\prime}\left[\frac{3}{64} + \frac{(1-2\nu)}{192}\cos 2\theta\right].
\end{aligned}
\tag{11}
$$

It is noted that the superscript comma(s) at the coefficient functions denote the derivative(s) of coefficient functions with respects to z. After loading and boundary conditions are imposed, the coefficient functions can be determined. It should be pointed out that the first set of the coefficient functions (a_{01}, b_{01} and b_{02}) provide the rigid body translations for the crack body. The second set of the coefficient functions (a_{12}, b_{11} and b_{12}) associate with the $\sqrt{r}$ expression for the displacements that account for the singularity at the crack front. Therefore the relationships between the stress intensity factors ($\mathbf{K}_{\mathrm{I}}$, $\mathbf{K}_{\mathrm{II}}$ and $\mathbf{K}_{\mathrm{III}}$) and the coefficient functions are

$$b_{11} = \frac{\mathbf{K}_{\mathrm{I}}}{\sqrt{2\pi}}, \quad b_{12} = \frac{\mathbf{K}_{\mathrm{II}}}{\sqrt{2\pi}} \quad \text{and} \quad a_{12} = \frac{\mathbf{K}_{\mathrm{III}}}{\sqrt{2\pi}} \tag{12}$$

The whole problem is reduced to the determination of the second set of coefficient functions.

2.2. Global interpolation function

Using eigenfunctions expansion technique and selecting the cylindrical coordinate system, the displacements which is close to the crack front have been expressed in a series form in equation(11). In order to compile with the global rectangle coordinate system, the displacements (u_r, v_θ, w_z) should be transformed to the nodal displacement (u, v, w) i.e.,

$$\begin{pmatrix} u \\ v \\ w \end{pmatrix} = \begin{bmatrix} \cos\theta & -\sin\theta & 0 \\ \sin\theta & \cos\theta & 0 \\ 0 & 0 & 1 \end{bmatrix} \begin{pmatrix} u_r \\ v_\theta \\ w_z \end{pmatrix}. \tag{13}$$

Assume the coefficient functions (a_{n1}, b_{n1} *and* c_{n1}) are quadratic, such that,

$$a_{ni}(z) = \sum_{j=1}^{3} N_j(z) a_{ni}^{(j)}\ ,\ b_{ni}(z) = \sum_{j=1}^{3} N_j(z) b_{ni}^{(j)}\ ,\text{and}\ c_{ni}(z) = \sum_{j=1}^{3} N_j(z) c_{ni}^{(j)}\ . \tag{14}$$

where $a_{ni}^{(j)}, b_{ni}^{(j)}$ and $c_{ni}^{(j)}$ are the nodal values of coefficient functions and $N_j(z)$ are the Lagrangian shape functions.

In the case of the same spacing between the nodes of element in z direction, and the coefficient functions are evaluate at the nodes of (x,y,z_1), (x,y,z_2) and (x,y,z_3), the coefficient functions for a_{ni} (z) becomes,

$$\begin{pmatrix} a_{ni}(z_1) \\ a_{ni}(z_2) \\ a_{ni}(z_3) \end{pmatrix} = \begin{bmatrix} 1 & 0 & 0 \\ 0 & 1 & 0 \\ 0 & 0 & 1 \end{bmatrix} \begin{pmatrix} a_{ni}^1 \\ a_{ni}^2 \\ a_{ni}^3 \end{pmatrix}. \tag{15}$$

We neglected the first and higher order derivatives, as the inter-element of usual solid finite element is C_0 continuity.

By substituting equations (11) into (8), the displacements characterized the singular stress field can be determined. Again, by making use of equation (15) and then equation (13) to transform the cylindrical coordinates to Cartesian coordinates the nodal displacement vector **d** can be expressed in terms of the nodal coefficient vector **a**,

$$\mathbf{d} = \mathbf{T}\mathbf{a} \tag{16}$$

where **T** is the global transformation matrix that associate with the coefficient functions. The form of the transformation matrix **T** can be illustrated by considering their column vectors. For the *n*-th transformation terms, the *m*-th component of the column vectors $\mathbf{T}_n$ of transformation matrix **T** is

$$T_{mn} = r^{n/2} F_{mn}(\theta), \tag{17}$$

where *r* is the perpendicular distances from the crack border to the corresponding node of element, $F_{mn}(\theta)$ is the function which is derived from the displacement functions (11) together with equations (13) and (15).

3. FRACTAL TWO LEVEL FINITE ELEMENT FOR 3-D CRACK PROBLEM

The FFEM is based on the separation of the sub-domain **D** that contains the singularity from the cracked solid by an artificial surface boundary $\mathbf{\Gamma}_o$ as shown in Figure1. Within **D** the solution is obtained by the FFEM on one hand, and outside **D** the solution is obtained by conventional FEM on the other hand.

3.1. Decomposition of stiffness for three-dimensional elements

Consider a *m*-node three-dimensional element, with an isoparametric form of relationship, the shape functions and the displacement functions may be expressed by

$$x = \sum_{i=1}^{m} N_i(\xi,\eta,\zeta)x_i \ , \ y = \sum_{i=1}^{m} N_i(\xi,\eta,\zeta)y_i \ \text{ and } \ z = \sum_{i=1}^{m} N_i(\xi,\eta,\zeta)z_i \tag{18}$$

and

$$u = \sum_{i=1}^{m} N_i(\xi,\eta,\zeta)u_i \ , \ v = \sum_{i=1}^{m} N_i(\xi,\eta,\zeta)v_i \ \text{ and } \ w = \sum_{i=1}^{m} N_i(\xi,\eta,\zeta)w_i \tag{19}$$

where (x_i, y_i, z_i) and (u_i, v_i, w_i) are the nodal coordinates and nodal displacements of an element respectively and $N_i(\xi,\eta,\zeta)$ are the shape functions. The associated stiffness matrix [**K**] is then calculated by

$$[\mathbf{K}] = \int_{-\mathbf{1}}^{\mathbf{1}}\int_{-1}^{1}\int_{-1}^{1}[\mathbf{B}]^{\mathbf{t}}[\mathbf{D}][\mathbf{B}]\mathbf{det}[\mathbf{J}]d\xi d\eta d\zeta \tag{20}$$

where

$$[\mathbf{B}] = \begin{bmatrix} \frac{\partial \mathbf{N}}{\partial x} & 0 & 0 \\ 0 & \frac{\partial \mathbf{N}}{\partial y} & 0 \\ 0 & 0 & \frac{\partial \mathbf{N}}{\partial z} \\ \frac{\partial \mathbf{N}}{\partial y} & \frac{\partial \mathbf{N}}{\partial x} & 0 \\ 0 & \frac{\partial \mathbf{N}}{\partial z} & \frac{\partial \mathbf{N}}{\partial y} \\ \frac{\partial \mathbf{N}}{\partial z} & 0 & \frac{\partial \mathbf{N}}{\partial x} \end{bmatrix} \tag{21}$$

$$[\mathbf{J}] = \begin{bmatrix} \frac{\partial x}{\partial \xi} & \frac{\partial y}{\partial \xi} & \frac{\partial z}{\partial \xi} \\ \frac{\partial x}{\partial \eta} & \frac{\partial y}{\partial \eta} & \frac{\partial z}{\partial \eta} \\ \frac{\partial x}{\partial \zeta} & \frac{\partial y}{\partial \zeta} & \frac{\partial z}{\partial \zeta} \end{bmatrix} \tag{22}$$

$$[\mathbf{D}] = \begin{bmatrix} \varepsilon & \lambda & \lambda & & & \\ \lambda & \varepsilon & \lambda & & \mathbf{0} & \\ \lambda & \lambda & \varepsilon & & & \\ & & & \mu & & \\ & \mathbf{0} & & & \mu & \\ & & & & & \mu \end{bmatrix} \tag{23}$$

where λ and μ are Lame's coefficients and ε is equal to $\lambda(1-\nu)/\nu$.

Considering two elements denoted by *1* and *2*, which are similar in *x* and *y* directions but remains the same in *z* direction such that

$x_i^2 = \alpha x_i^1$, $y_i^2 = \alpha y_i^1$ and $z_i^2 = z_i^1$.

Therefore, by equation (22), one can have

$$\mathbf{det}[\mathbf{J}]_2 = \alpha^2 \mathbf{det}[\mathbf{J}]_1 . \tag{24}$$

The stiffness matrix [**K**] of equation (20) for element *2* can be decomposed according to the power of α to three sub-matrices $[\mathbf{S}]_0$, $[\mathbf{S}]_1$ and $[\mathbf{S}]_2$, such that

$$[\mathbf{K}]_2 = \int_{-\mathbf{1}}^{\mathbf{1}}\int_{-1}^{1}\int_{-1}^{1}[\mathbf{B}]_2^t[\mathbf{D}][\mathbf{B}]_2 \mathbf{det}[\mathbf{J}]_2 d\xi d\eta d\zeta = [\mathbf{S}]_0 + \alpha[\mathbf{S}]_1 + \alpha^2[\mathbf{S}]_\mathbf{2} . \tag{25}$$

where

$$[\mathbf{S}]_0 = \int_{-1}^{1}\int_{-1}^{1}\int_{-1}^{1} \begin{bmatrix} \varepsilon\frac{\partial \mathbf{N}^t}{\partial x}\frac{\partial \mathbf{N}}{\partial x} + \mu\frac{\partial \mathbf{N}^t}{\partial y}\frac{\partial \mathbf{N}}{\partial y} & \lambda\frac{\partial \mathbf{N}^t}{\partial x}\frac{\partial \mathbf{N}}{\partial y} + \mu\frac{\partial \mathbf{N}^t}{\partial y}\frac{\partial \mathbf{N}}{\partial x} & \mathbf{0} \\ \lambda\frac{\partial \mathbf{N}^t}{\partial y}\frac{\partial \mathbf{N}}{\partial x} + \mu\frac{\partial \mathbf{N}^t}{\partial x}\frac{\partial \mathbf{N}}{\partial y} & \mu\frac{\partial \mathbf{N}^t}{\partial x}\frac{\partial \mathbf{N}}{\partial x} + \varepsilon\frac{\partial \mathbf{N}^t}{\partial y}\frac{\partial \mathbf{N}}{\partial y} & \mathbf{0} \\ \mathbf{0} & \mathbf{0} & \mu\frac{\partial \mathbf{N}^t}{\partial x}\frac{\partial \mathbf{N}}{\partial x} + \mu\frac{\partial \mathbf{N}^t}{\partial y}\frac{\partial \mathbf{N}}{\partial y} \end{bmatrix} \mathbf{det}[\mathbf{J}]_1 \, d\xi d\eta d\zeta \tag{26}$$

$$[\mathbf{S}]_1 = \int_{-1}^{1}\int_{-1}^{1}\int_{-1}^{1} \begin{bmatrix} \mathbf{0} & \mathbf{0} & \lambda\frac{\partial \mathbf{N}^t}{\partial x}\frac{\partial \mathbf{N}}{\partial z} + \mu\frac{\partial \mathbf{N}^t}{\partial z}\frac{\partial \mathbf{N}}{\partial x} \\ \mathbf{0} & \mathbf{0} & \lambda\frac{\partial \mathbf{N}^t}{\partial y}\frac{\partial \mathbf{N}}{\partial z} + \mu\frac{\partial \mathbf{N}^t}{\partial z}\frac{\partial \mathbf{N}}{\partial y} \\ \lambda\frac{\partial \mathbf{N}^t}{\partial z}\frac{\partial \mathbf{N}}{\partial x} + \mu\frac{\partial \mathbf{N}^t}{\partial x}\frac{\partial \mathbf{N}}{\partial z} & \lambda\frac{\partial \mathbf{N}^t}{\partial z}\frac{\partial \mathbf{N}}{\partial y} + \mu\frac{\partial \mathbf{N}^t}{\partial y}\frac{\partial \mathbf{N}}{\partial z} & \mathbf{0} \end{bmatrix} \mathbf{det}[\mathbf{J}]_1 \, d\xi d\eta d\zeta \tag{27}$$

and

$$[\mathbf{S}]_2 = \int_{-1}^{1}\int_{-1}^{1}\int_{-1}^{1} \begin{bmatrix} \mu\frac{\partial \mathbf{N}^t}{\partial z}\frac{\partial \mathbf{N}}{\partial z} & \mathbf{0} & \mathbf{0} \\ \mathbf{0} & \mu\frac{\partial \mathbf{N}^t}{\partial z}\frac{\partial \mathbf{N}}{\partial z} & \mathbf{0} \\ \mathbf{0} & \mathbf{0} & \varepsilon\frac{\partial \mathbf{N}^t}{\partial z}\frac{\partial \mathbf{N}}{\partial z} \end{bmatrix} \mathbf{det}[\mathbf{J}]_1 \, d\xi d\eta d\zeta \, . \tag{28}$$

The equation (25) can be used to calculate any element stiffness matrix with similar shape on the *x*-*y* plane.

3.2. Fractal transformation

Finally the generalized stiffness matrix in domain **D** can be determined by transforming the stiffness matrix of the first layer of mesh as shown in Figure 2 and modifying each entry of the stiffness matrix.

For the first layer of mesh, let the displacements on the boundary Γ_o be the masters $\mathbf{u}_m$ and the displacements within the boundary Γ_o be the slaves $\mathbf{u}_s$. To carry out the transformation, the stiffness matrix [**K**] in equation (21) is first partitioned with respect to the master and slaves displacements,

$$[\mathbf{K}](\mathbf{d}) = \begin{bmatrix} \mathbf{K}_{ss}^{f} & \mathbf{K}_{sm}^{f} \\ \mathbf{K}_{ms}^{f} & \mathbf{K}_{mm}^{f} \end{bmatrix} \begin{pmatrix} \mathbf{u}_s \\ \mathbf{u}_m \end{pmatrix} \tag{29}$$

where the superscript '*f*' indicates first layer of mesh. Only the displacements at the slaves are transformed. Second level (global) interpolation of displacements can be written as follows,

$$\begin{pmatrix} \mathbf{u}_s \\ \mathbf{u}_m \end{pmatrix} = \begin{bmatrix} \mathbf{T} & \mathbf{0} \\ \mathbf{0} & \mathbf{I} \end{bmatrix} \begin{pmatrix} \mathbf{a} \\ \mathbf{u}_m \end{pmatrix} \tag{30}$$

After transformation, we have,

$$\begin{bmatrix} \mathbf{T}^t \mathbf{K}_{ss}^{f} \mathbf{T} & \mathbf{T}^t \mathbf{K}_{sm}^{f} \\ \mathbf{K}_{ms}^{f} \mathbf{T} & \mathbf{K}_{mm}^{f} \end{bmatrix} \begin{pmatrix} \mathbf{a} \\ \mathbf{u}_m \end{pmatrix} = \begin{pmatrix} \mathbf{0} \\ \mathbf{0} \end{pmatrix} \tag{31}$$

For the inner layer, each element stiffness matrix within the first layer of **D** would be transformed and assembled to form the global stiffness matrix. Based on the concept of fractal mesh generation around the crack tip, infinite number of elements and numerous degrees of freedom would be generated. However applying the fast transformation technique, infinite many layers of mesh can be transformed and assembled.

Utilising equations (16) and (25), the inner *k*-th layer of element stiffness is transforming and assembling,

$$\begin{aligned} \sum_{k=2}^{\infty} \mathbf{K}_k &= \sum_{k=2}^{\infty} \mathbf{T}^{kt} [\mathbf{S}_0 + \alpha^{(k-1)} \mathbf{S}_1 + \alpha^{2(k-1)} \mathbf{S}_2] \mathbf{T}^k \mathbf{a} \\ &= \sum_{k=2}^{\infty} \sum_{j=0}^{2} \alpha^{j(k-1)} \mathbf{T}^{kt} \mathbf{S}_j \mathbf{T}^k \mathbf{a} \quad \text{and} \quad \alpha = \tfrac{1}{2}. \end{aligned} \tag{32}$$

The above equation can be rewritten as

$$\sum_{k=2}^{\infty} \mathbf{K}_k = \sum_{j=0}^{2} \sum_{k=0}^{\infty} \alpha^{j(k-1)} \mathbf{T}^{kt} \mathbf{S}_j \mathbf{T}^k \mathbf{a} \tag{33}$$

Recalling equation (17) that r^k can be written as $\alpha^{k-1}r^f$ for the *m*-th component of the *n*-th column vector $\mathbf{T}_n^k$ of the transformation matrix $\mathbf{T}^k$. The column vector $\mathbf{T}_n^k$ at the *k*-th layer corresponding to the *n*-th transformation term can be therefore related to that of the first layer,

$$\mathbf{T}_n^k = \alpha^{(k-1)\frac{n}{2}}\mathbf{T}_n^f \ . \tag{34}$$

Similarly, all the sub-matrices $\mathbf{E}_{mn}^{kj}$ (at *m*-th and *n*-th entry) in $\alpha^{j(k-1)}\mathbf{T}^{kt}\mathbf{S}_j\mathbf{T}^k$ (*k*=0 to ∞, *j*=0 to 2) of equation (33) can then be related to the first layer, such that

$$\mathbf{E}_{mn}^{kj} = \alpha^{j(k-1)}\mathbf{T}_m^{kt}\mathbf{S}_j\mathbf{T}_n^k = [\alpha^{(m+n+2j)/2}]^{k-1}\mathbf{T}_m^{ft}\mathbf{S}_j\mathbf{T}_n^f = [\alpha^{(m+n+2j)/2}]^{k-1}\mathbf{E}_{mn}^{fj} \tag{35}$$

The infinite sum of equation (35) is a geometric series, hence, the infinite series can be simplified and expressed as

$$\sum_{k=2}^{\infty}\mathbf{E}_{mn}^{kj} = \frac{\psi_{mnj}}{1-\psi_{mnj}}\mathbf{E}_{mn}^{fj} \ ; \qquad \psi_{mnj} = \alpha^{(m+n+2j)/2} \tag{36}$$

The stiffness matrices of infinite layer of inner meshes are then calculated by making use of equations(33) and (36). A program listing of the subroutine of fast transformation procedure is shown in Appendix A.

4. NUMERICAL EXAMPLES

In order to demonstrate the accuracy and the efficiency that can be attained by using FFEM, the present section reports the results obtained from the analysis of a few cases for which the analytical solution is known. All the Young's modulus and Poisson's ratio is assumed to be 20000 units and 0.3 respectively.

4.1. Single edge crack tension

A cracked plate known as single edge crack in tension is considered in this example. It is a two-dimensional pure mode I plane strain problem. A layer of three-dimensional finite element meshes for ratio of crack length per width (*a/w*) of 0.3 used for the analysis is shown in Figure 3. Due to symmetry, only half of the specimen is analysed, the total number of elements is 15 and the total number of unknowns is 738. Three-dimensional Lagrangian elements with full Guassian integration scheme used throughout. The maximum computational time is 330 seconds by a PC modelled 486 in 66MHz. In order to model the plane strain situation, all the boundary nodal displacements in *z*-direction are prescribed to

zero. The dimensionless stress intensity factors $\mathbf{K}_{\mathrm{I}}/(\sigma\sqrt{\pi a})$ are tabulated in Table 1. Present results give very good agreements with less than 2% different with Ref[19] and reproduce the 'same' results as two-dimensional fractal finite element method[20].

a/*w*	Present	Ref[19]	FFEM (2-D)
0.1	1.172	1.184	1.171
0.2	1.354	1.371	1.355
0.3	1.643	1.660	1.643
0.4	2.082	2.104	2.082
0.5	2.786	2.826	2.787
0.6	3.966	4.026	3.966

Table.1 Dimensionless stress intensity factors for single edge crack tension

4.2. Single edge crack shear

A cracked plate subjected to a pair of equal and opposite point loads Q at x-direction at the crack faces is considered in this example. It is a pure mode II plane strain problem. The dimensionless stress intensity factors $\mathbf{K}_{\mathrm{II}}\sqrt{\pi a}/(2Q)$ for various orders of transformation terms are listed in Table 2. It is shown that the maximum percentage difference of the present result when compared with Ref[19] is 3%. Furthermore, two-dimensional [20] and three-dimensional FFEM give the 'same' results.

a/*w*	Present	Ref[19]	FFEM (2-D)
0.1	1.302	1.306	1.296
0.2	1.314	1.327	1.313
0.3	1.342	1.370	1.342
0.4	1.414	1.442	1.413
0.5	1.513	1.559	1.513
0.6	1.697	1.745	1.696

Table.2 Dimensionless stress intensity factors for single edge crack shear

4.3. Pure mode I semi-infinite plane crack

In most instances, crack is subject to a state of tri-axial stress. In order to demonstrate the accuracy and convenience of using present method to calculate three-dimensional cracks, the simple crack geometry of semi-infinite plane subject to a point load P_y at the Cartesian coordinate (-1, 0, 0) is chosen here. The geometry of crack, loading arrangement and the coordinates system are shown in Figure 4. It is a pure mode I three-dimensional crack problem. The exact solution was found by Sih and Kassir [21] making use of integral transformation method. The SIF is expressed as,

$$\mathbf{K}_{\mathrm{I}} = \frac{2^{1/2} P_y}{\pi^{3/2}} \frac{a^{1/2}}{a^2 + z^2} \tag{37}$$

where P_y =1 is the applied point load at x=-a in the xz plane.

As it is not possible to model the infinite domain by the convenient finite element method, a cracked cylinder with radius 32units and width 64 units is considered here. A one out of eight non-uniform-thickness layer of finite element meshes is shown in Figure 5, there are totally 324 elements and corresponding to 3648 nodes. The results obtained by the present method together with the exact solution are shown in Figure 6. The maximum value of SIF at z=0 equal to 0.2575 and 0.2540 for the present result and the theoretical value respectively. Very good agreement is obtained. In addition, the present method is programmed by FORTRAN language by using single precision and double precision manner. The resulting SIFs agree up to four significant figures that indicate the present scheme is numerically stable.

4.4. Mixed modes semi-infinite plane crack

By replacing the applied loading P_y to P_x in the above example, the problem considered here becomes a second and third modes mixed problem. The exact solution was determined by Sih and Kassir [21],

$$\mathbf{K}_{\mathrm{II}} = \frac{2^{1/2} P_x}{(a\pi)^{3/2}} \left(\frac{1}{1+z_0^2} \right) \left[1 + \left(\frac{2\nu}{2-\nu} \right) \frac{1-z_0^2}{1+z_0^2} \right] \tag{38}$$

$$\mathbf{K}_{\mathrm{III}} = \frac{2^{1/2} P_x}{(\pi a)^{3/2}} \left(\frac{4\nu}{2-\nu} \right) \frac{z_0}{(1+z_0^2)^2} \tag{39}$$

where $z_0 = z/a$. The stress intensity factor determined by the present method together with the exact solution are plotted in Figure 7, the maximum value of SIFs for mode II and mode III

by the present method is 0.3477 and 0.0597 respectively, whereas the corresponding exact values is 0.3436 and 0.0582. Very good accuracy is achieved by the present method.

5. CONCLUSION

Fractal finite element method was presented for the determination of SIFs for the straight three-dimenisonal plane crack. The analytical displacement eigenfunction for straight semi-infinite plane crack are derived up to the eighth terms. Moreover, the use of fractal geometry concept to generate infinite many of finite elements around the crack border was introduced. Applying the newly developed fast transformation technique, numerous DOFs around the crack border were transformed to a small set of generalised coordinates. And the SIFs can be evaluated directly from the generalised coordinates. Thus no post-processing techniques are required to extract the SIFs. Four examples on pure mode I, pure mode II and mixed modes cracks were given to demonstrate the accuracy and efficiency of the present method. Very good accuracy with less than 3% errors is obtained for the maximum value of SIFs for different modes.

ACKNOWLEDGEMENT

The work described in this paper was fully supported by the grants from the Research Grants Council of the Hong Kong Special Administrative Region, China (Project Nos. HKU 7014/00E and CityU 1047/00E).

REFERENCES

1. C. M. Hudson and T. P. Rich, *Case Histories Involving Fatigue and Fracture Mechanics*. ASTM STP 918, (1986).
2. D. R. J. Owen and A. J. Fawkes, *Engineering Fracture Mechanics: Numerical Methods and Application*, Pineridge Press Ltd., Swansea, U.K., (1983).
3. S. N. Atluri, *Computational Methods in Mechanics of Fracture*. North-Holland, Amsterdam (1986).

4. M. H. Aliabadi and D. P. Rooke, *Numerical Fracture Mechanics*, Computational Mechanics, Southampton, U.K. (1991).
5. J. R. Rice, A path independent integral and the approximate analysis of strain concentration by Notches and cracks. *J.l Appl. Mech.*, **35**, 379-386 (1968).
6. H. G. deLorenzi, On the energy release rate and the J-integral for 3-D crack configurations, *Int. J. Frac. Mech.,* **19**, 183-193 (1982).
7. H. A. Sosa, On the analysis of bars, beams and plates with defects. Ph.D. thesis, Stanford University (1986).
8. T. K. Hellen, On the method of virtual crack extensions. *Int. J. Numer. Method Engng.* **9**, 187-207 (1975).
9. K. N. Shivakumar and I. S. Raju, An equivalent domain integral method for three-dimensional mixed-mode fracture problems. *Engng. Frac. Mech.* **42**, No.6, 935-959 (1992).
10. K. N. Shivakumar, P. W. Tan and J. C. Newman, Virtual crack closure technique for calculating stress-intensity factors for cracked three-dimensional bodies. *Int. J. Frac.* **36**, R43-R50 (1988).
11. X. Niu and G. Glinka, Stress intensity factors for semi-elliptical surface cracks in welded joints. *Int. J. Frac.* **40**, 255-270 (1989).
12. R. Bains, M. H. Aliabadi and D. P. Rooke, Stress intensity factor weight functions for cracks in 3-D finite geometries. *Advances in Boundary Element Methods for Fracture Mechanics*, (Editors: M. H. Aliabadi and C. A. Brebbia), 201-268, Elsevier Applied Science, London (1993).
13. T. Nishioka and S. N. Atluri, An alternating method for analysis of surface flawed aircraft structural components. *AIAA J.* **21**, 749-757 (1983).
14. Y. Long and Q. Jun, Calculation of stress intensity factors for surface cracks in a three-dimensional body by the sub-region mixed FEM. *Comp. Struc.* **44**, No.1/2, 75-78 (1992).
15. M. L. Luchi and S. Rizzuti, Special crack-tip elements for 3-D problems. *Advances in Boundary Element Methods for Fracture Mechanics*, (Editors: M. H. Aliabadi and C. A. Brebbia), 173-200, Elsevier Applied Science, London (1993).
16. A.Y.T. Leung and R. K. L. Su, Fractal two-level finite element methods for 2-D crack problems. *Proc. 2nd Asian-Pacific Conf. on Computational Mechanics*, A. A. Balkema/Rotterdam/ brookfield, 675-679 (1993).

17. A.Y.T. Leung and R.K.L. Su, Mode I crack problems by fractal two level finite element methods, *Engng. Frac. Mech.* **48**(6), p847-856.
18. R. J. Hartranft and G. C, Sih, The use of eigenfunction expansions in the general solution of three-dimensional crack problems, *J. Math. Mech.* **19**, No.2, 123-138 (1969).
19. Y. Murakami, *Stress Intensity Factors Handbook*, Pergamon Press (1987).
20. A. Y. T. Leung and R. K. L. Su, Applications of fractal two-level finite element method of 2-D cracks, *Microcomputers in Civil Engineering,* **11**(4), p249-257.
21. G. C. Sih and M. K. Kassir, Mechanics of Fracture Vol.2 Three-dimensional crack problems, Academic Press, New York, (1975).

APPENDIX A

Program listing for fast transformation

```
      SUBROUTINE FAST(TEMP,IFACT)                                       FAST   1
C*********************************************************************FAST   2
C                                                                       FAST   3
C*** SUBROUTINE FOR FAST TRANSFORMATION OF EACH TERM IN THE TEMP MATRIX FAST   4
C     IFACT = THE NO. OF SUB-MATRIX RANGED FROM 1 TO 3 OF EQN (25)      FAST   5
C                                                                       FAST   6
C*********************************************************************FAST   7
      IMPLICIT DOUBLE PRECISION(A-H,O-Z)                                FAST   8
      DIMENSION TEMP(81,81)                                             FAST   9
      IF(IFACT.EQ.1) L=0                                                FAST  10
      IF(IFACT.EQ.2) L=2                                                FAST  11
      IF(IFACT.EQ.3) L=4                                                FAST  12
      DO 10 J=1,9                                                       FAST  13
      J1=(J-1)*3                                                        FAST  14
      J2=(J+5)*3                                                        FAST  15
      J3=(J+11)*3                                                       FAST  16
      IF(J.GE.7) THEN                                                   FAST  17
      J1=(J+11)*3                                                       FAST  18
      J2=(J+14)*3                                                       FAST  19
      J3=(J+17)*3                                                       FAST  20
      ENDIF                                                             FAST  21
      DO 10 I=1,9                                                       FAST  22
      I1=(I-1)*3                                                        FAST  23
      I2=(I+5)*3                                                        FAST  24
      I3=(I+11)*3                                                       FAST  25
      IF(I.GE.7) THEN                                                   FAST  26
      I1=(I+11)*3                                                       FAST  27
      I2=(I+14)*3                                                       FAST  28
      I3=(I+17)*3                                                       FAST  29
      ENDIF                                                             FAST  30
      R=0.5D0**(FLOAT(I+J+L-2)/2.0D0)                                   FAST  31
C                                                                       FAST  32
C*** EVALUATION OF THE GEOMETRIC SERIES                                 FAST  33
C                                                                       FAST  34
      F=R/(1.D0-R)                                                      FAST  35
      DO 10 IDIME=1,3                                                   FAST  36
      DO 10 JDIME=1,3                                                   FAST  37
      TEMP(I1+IDIME,J1+JDIME)=F*TEMP(I1+IDIME,J1+JDIME)                 FAST  38
      TEMP(I1+IDIME,J2+JDIME)=F*TEMP(I1+IDIME,J2+JDIME)                 FAST  39
      TEMP(I1+IDIME,J3+JDIME)=F*TEMP(I1+IDIME,J3+JDIME)                 FAST  40
      TEMP(I2+IDIME,J1+JDIME)=F*TEMP(I2+IDIME,J1+JDIME)                 FAST  41
      TEMP(I2+IDIME,J2+JDIME)=F*TEMP(I2+IDIME,J2+JDIME)                 FAST  42
      TEMP(I2+IDIME,J3+JDIME)=F*TEMP(I2+IDIME,J3+JDIME)                 FAST  43
      TEMP(I3+IDIME,J1+JDIME)=F*TEMP(I3+IDIME,J1+JDIME)                 FAST  44
      TEMP(I3+IDIME,J2+JDIME)=F*TEMP(I3+IDIME,J2+JDIME)                 FAST  45
   10 TEMP(I3+IDIME,J3+JDIME)=F*TEMP(I3+IDIME,J3+JDIME)                 FAST  46
      RETURN                                                            FAST  47
      END                                                               FAST  48
```

FIGURES

Figure 1. Singlular and regular regions

Figure 2. Construction of fractal mesh

Figure 3. Mesh Configuration os SECT (a/w = 0.3)

Figure 4. Semi-infinite straight plane crack (a =1.0)

Figure 5. A layer of 3-D finite element mesh

Figure 6. $\mathbf{K}_{\mathrm{I}}$ of semi-infinite plane crack subject to point loads

Figure 7. $\mathbf{K}_{\mathrm{I}}$ and $\mathbf{K}_{\mathrm{II}}$ of semi-infinite plane crack subject to shear loads

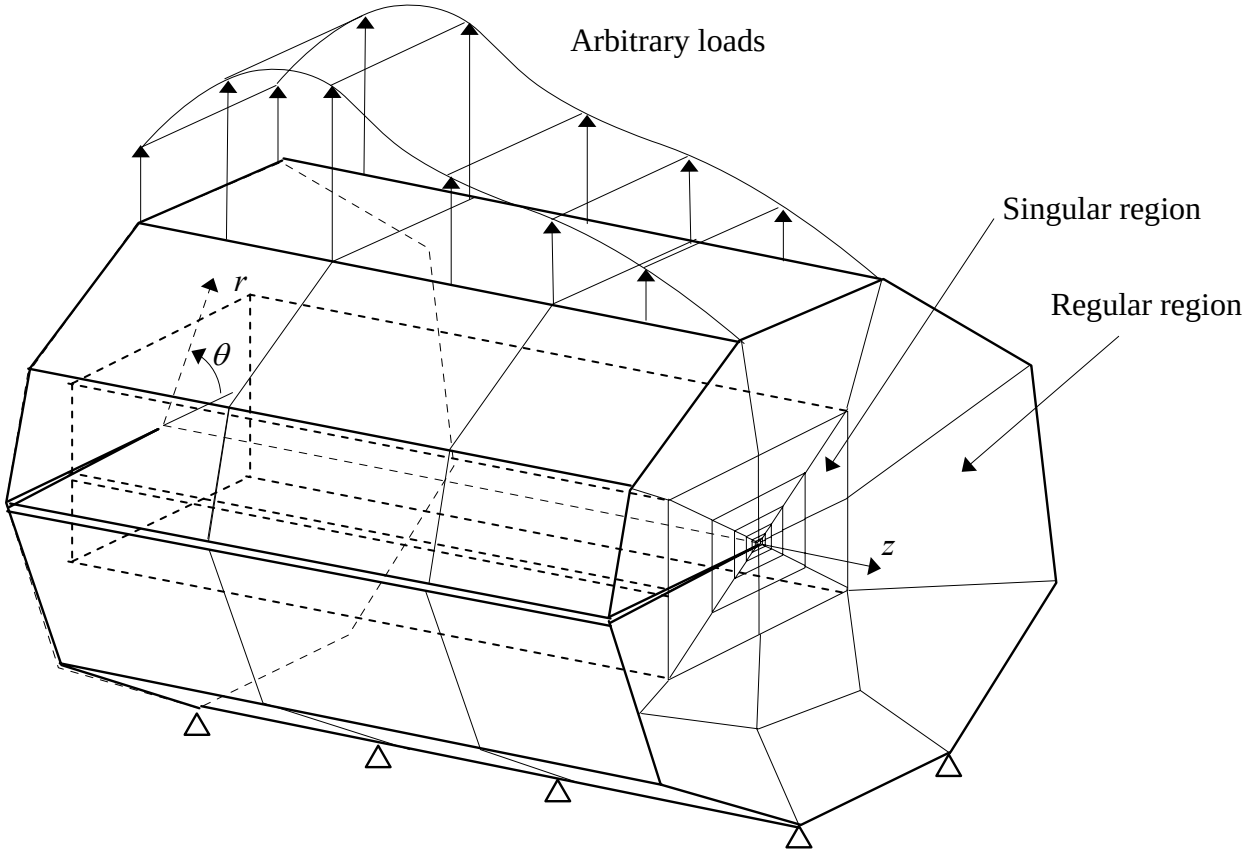

Figure 1. Singlular and regular regions

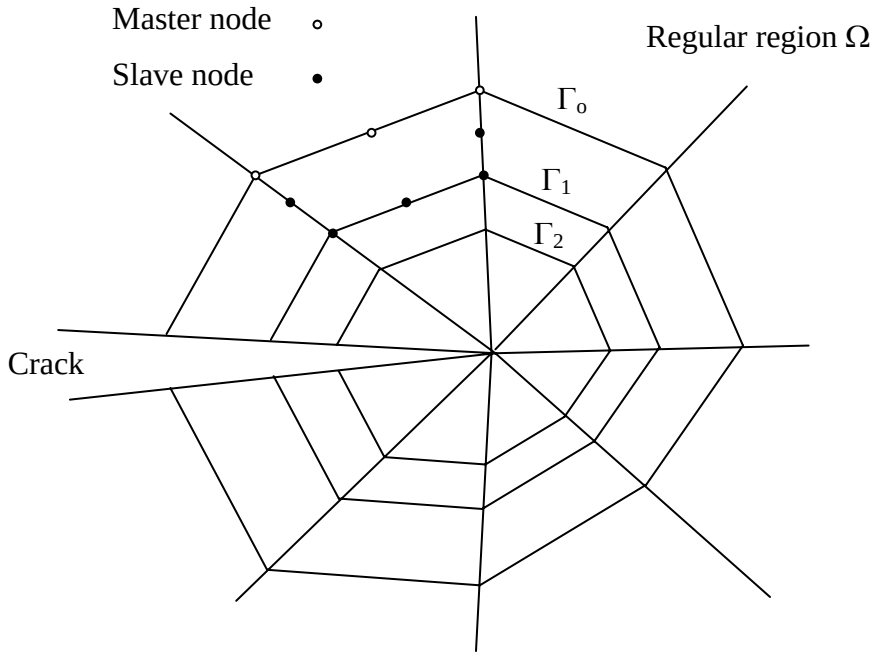

Figure 2. Construction of fractal mesh

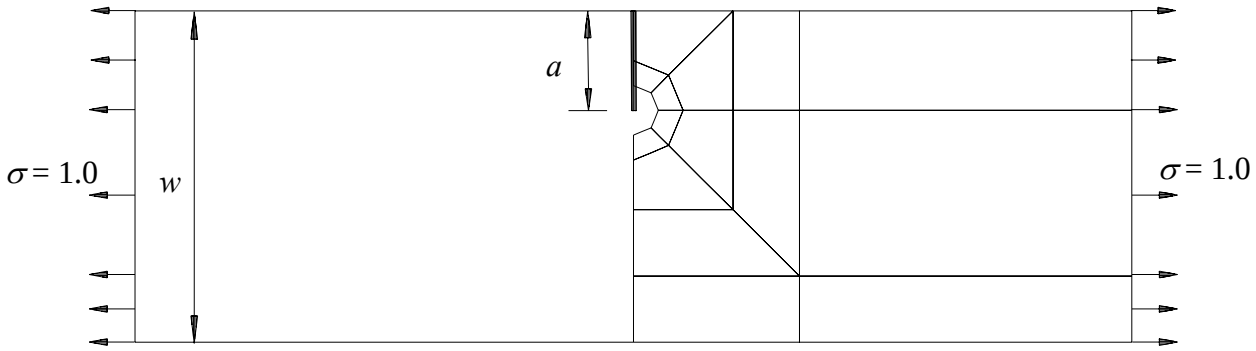

Figure 3. Mesh Configuration os SECT (a/w = 0.3)

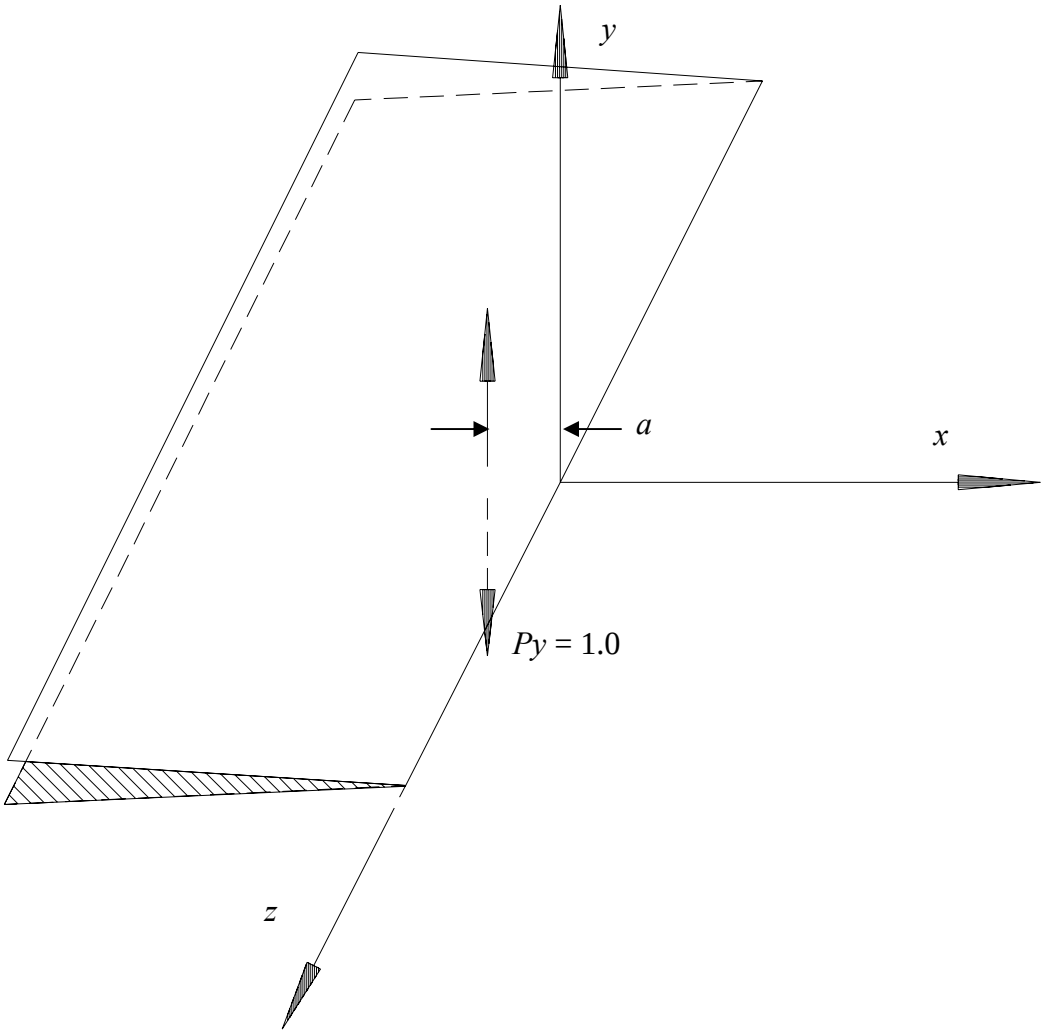

Figure 4. Semi-infinite straight plane crack (a =1.0)

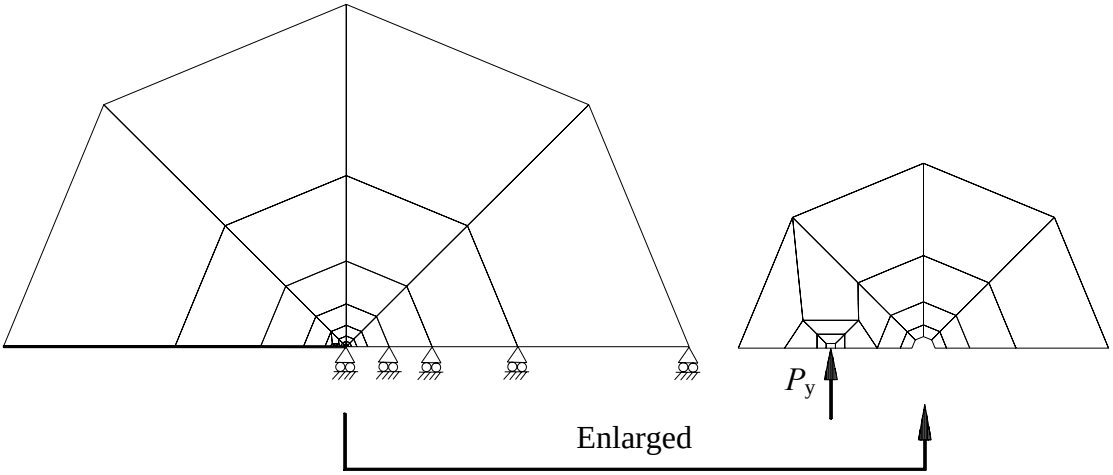

Figure 5. A layer of 3-D finite element mesh

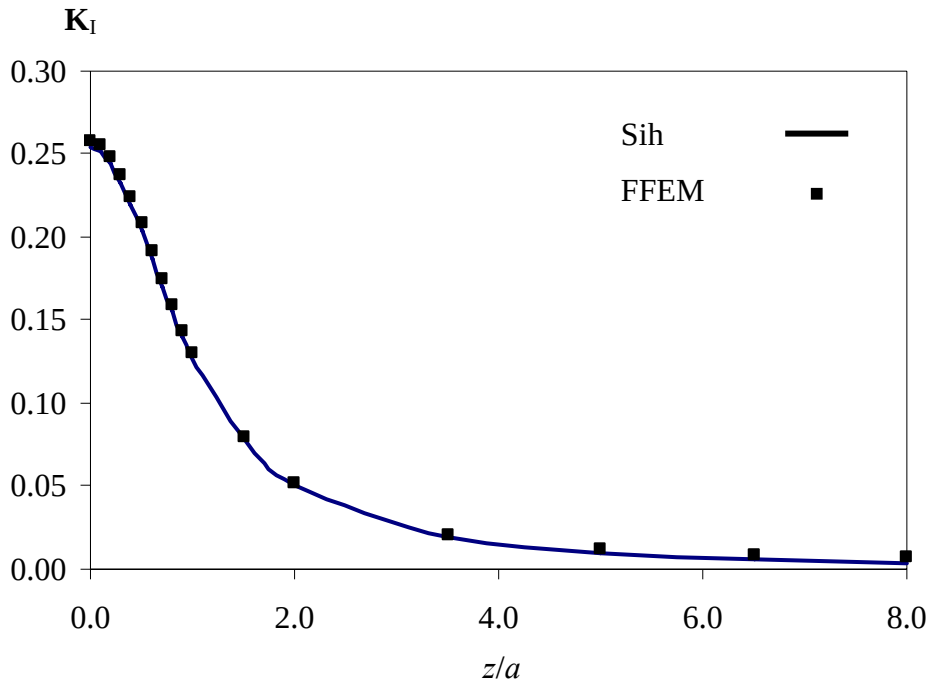

Figure 6. $\mathbf{K}_I$ of semi-infinite plane crack subject to point loads

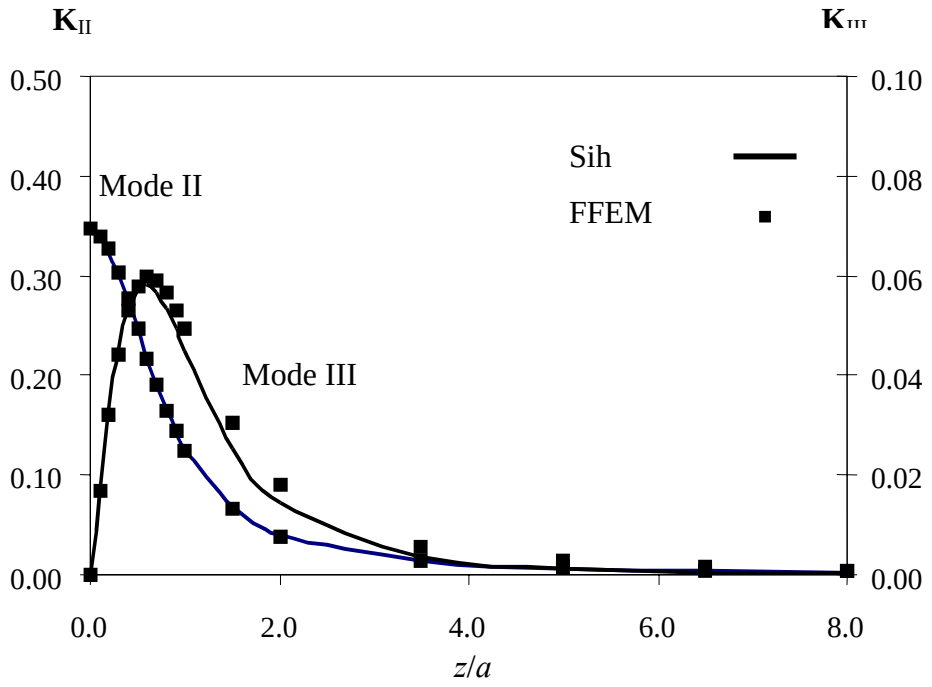

Figure 7. $\mathbf{K}_{I}$ and $\mathbf{K}_{II}$ of semi-infinite plane crack subject to shear loads